LETTERS

Glacial greenhouse-gas fluctuations controlled by ocean circulation changes

Andreas Schmittner[1] & Eric D. Galbraith[2]

Earth's climate and the concentrations of the atmospheric greenhouse gases carbon dioxide (CO_2) and nitrous oxide (N_2O) varied strongly on millennial timescales during past glacial periods. Large and rapid warming events in Greenland and the North Atlantic were followed by more gradual cooling, and are highly correlated with fluctuations of N_2O as recorded in ice cores. Antarctic temperature variations, on the other hand, were smaller and more gradual, showed warming during the Greenland cold phase and cooling while the North Atlantic was warm, and were highly correlated with fluctuations in CO_2. Abrupt changes in the Atlantic meridional overturning circulation (AMOC) have often been invoked to explain the physical characteristics of these Dansgaard–Oeschger climate oscillations[1–3], but the mechanisms for the greenhouse-gas variations and their linkage to the AMOC have remained unclear[4–8]. Here we present simulations with a coupled model of glacial climate and biogeochemical cycles, forced only with changes in the AMOC. The model simultaneously reproduces characteristic features of the Dansgaard–Oeschger temperature, as well as CO_2 and N_2O fluctuations. Despite significant changes in the land carbon inventory, CO_2 variations on millennial timescales are dominated by slow changes in the deep ocean inventory of biologically sequestered carbon and are correlated with Antarctic temperature and Southern Ocean stratification. In contrast, N_2O co-varies more rapidly with Greenland temperatures owing to fast adjustments of the thermocline oxygen budget. These results suggest that ocean circulation changes were the primary mechanism that drove glacial CO_2 and N_2O fluctuations on millennial timescales.

Our model simulates the coupled ocean–atmosphere–sea-ice–biosphere system[9]; it includes a dynamic terrestrial vegetation and carbon cycle model[10], and a three-dimensional ocean general circulation model with ocean ecosystem dynamics and cycling of nitrogen, phosphorous, oxygen and carbon. The model uses a simple, energy-balance atmosphere and was run under glacial conditions (Methods). The model is forced by varying idealized freshwater perturbations to the North Atlantic (Fig. 1), mimicking surrounding ice-sheet fluctuations. We note that the simulations are idealized, in that the true forcing behind Dansgaard–Oeschger (D-O) cycles remains unknown. The model forcing is thus arbitrary and was chosen only to trigger AMOC variations.

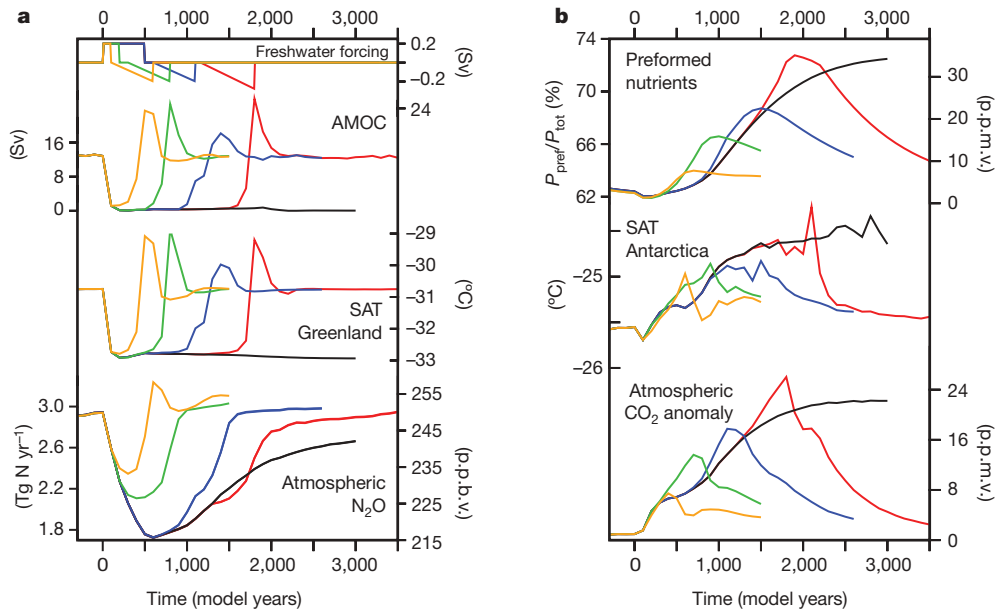

Figure 1 | Model simulations of glacial climate and greenhouse-gas fluctuations. The five model sensitivity runs differ in the length (yellow, 400 years; green, 700 years; blue, 1,100 years; and red, 1,700 years) of the simulated stadial (cold phase in Greenland). **a**, Time series of (from top) freshwater forcing, AMOC, Greenland surface air temperature (SAT), ocean N_2O production (left scale) and atmospheric N_2O concentration (right scale). **b**, Time series of global fraction of preformed nutrients (left scale) and corresponding changes in atmospheric p_{CO_2} according to the simple theory[22] (right scale), Antarctic SAT, and atmospheric CO_2 simulated by the complex model. Red lines correspond to the simulation shown in Figs 2 and 3.

[1]College of Oceanic & Atmospheric Sciences, Oregon State University, Corvallis, Oregon 97331, USA. [2]Atmospheric and Ocean Sciences, Princeton University, Princeton, New Jersey 08544, USA.

In response to the forcing, sinking of North Atlantic Deep Water (NADW) stops and the AMOC rapidly spins down from 13 Sv ($1\,Sv = 10^6\,m^3\,s^{-1}$) at model year 0 to almost 0 Sv after 100 years. Five sensitivity experiments have been conducted to assess the influence of the duration of the AMOC oscillations. In four experiments, the AMOC is switched back on after 400, 700, 1,100 and 1,700 years, respectively. In one experiment, it remains turned off (black lines, Fig. 1). The modelled climatic response, including rapid cooling in the North Atlantic and gradual warming in the Southern Hemisphere, is caused by reduced northward heat transport in the Atlantic, as described in detail elsewhere[11,12]. It is qualitatively consistent with reconstructions but quantitatively underestimates the surface air temperature changes over Greenland and Antarctica, presumably owing to missing atmospheric dynamics. The experiments were not designed to reproduce any particular observed event. We choose the time period from 50 to 45 kyr before present (BP) for the comparison in Fig. 2 because the duration of the stadial phase corresponds well to one of our experiments.

After the AMOC collapse (following year 0), marine N_2O production rapidly decreases by 40% to less than 1.8 Tg N yr^{-1} during year 600 (Fig. 1). Figure 3 shows that N_2O production decreases almost everywhere in the global ocean except for the North Atlantic. The decrease is largest in the low-oxygen regions of the eastern tropical Pacific and the northern Indian Ocean, but it is also noticeable in the North Pacific and elsewhere. Decreased productivity[13] and better ventilation of thermocline waters lead to increasing subsurface oxygen concentrations, reducing Indo-Pacific N_2O production[14]. Simulated N_2O concentrations co-vary strongly with Greenland temperatures with little time lag (~100 years), consistent with the palaeorecord[15]. Modelled N_2O amplitudes are 15–40 parts per billion by volume (p.p.b.v.), and larger over longer stadials. This is in excellent agreement with ice-core data[15] (Fig. 2 inset) and consistent with the earlier finding[15] that N_2O increases are larger for longer interstadials, which generally follow longer stadials (see also Supplementary Note). After the rapid contemporaneous increases in simulated Greenland temperatures and N_2O concentrations, they remain constant, in contrast to observations, owing to the idealized forcing applied (Supplementary Fig. 3) and the lack of atmospheric and ice-sheet variability. Despite this difference, the simulated N_2O concentrations and Greenland temperatures remain highly correlated, consistent with the observations.

The amplitude of our simulated N_2O variability is much larger than that found in a previous study (10 p.p.b.v.) that used a zonally averaged ocean model[8]. As noted above, the simulated N_2O production changes show a strong zonal structure and, together with the

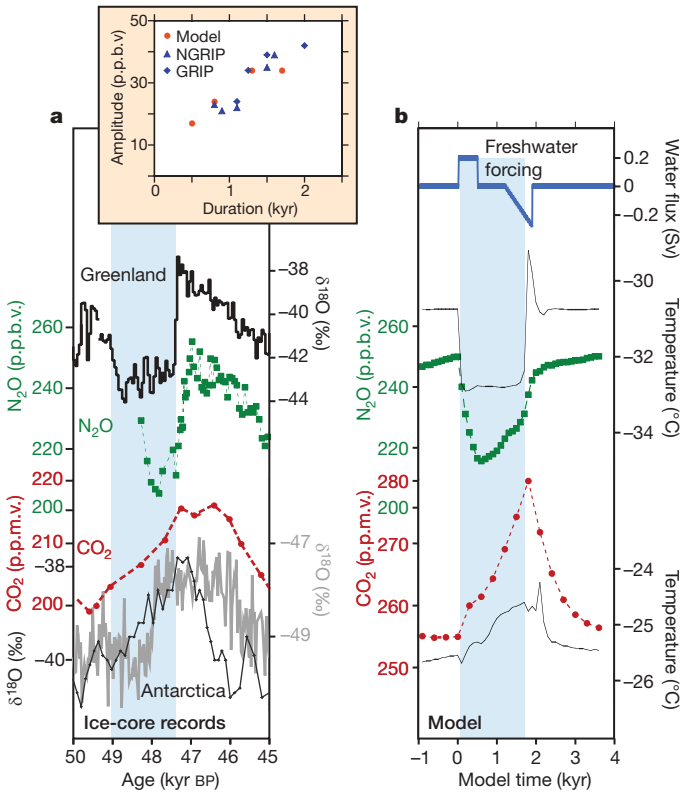

Figure 2 | Example of millennial changes in climate and greenhouse gases as recorded in polar ice cores from 45 to 50 kyr BP in comparison with model simulation. **a**, Ice-core records; **b**, model. Light blue shading indicates the stadial (cold in Greenland) phase following D-O interstadial 13 and immediately followed by rapid warming into D-O interstadial 12. This stadial coincides with an event of widespread ice-rafted debris in North Atlantic sediments (Heinrich event H5). In **a**, Greenland observations include $\delta^{18}O$ (ref. 28; temperature proxy) and N_2O concentrations[15]; Antarctic records include $\delta^{18}O$ (Dronning Maud Land[29], grey, and Byrd[17], black), and CO_2 (Taylor Dome[30]) on the age scale of ref. 24, shifted from the GISP2 age scale by 1.8 kyr to synchronize with the NGRIP age scale (Supplementary Information). In **b**, model output shows imposed North Atlantic freshwater forcing, temperature changes over Greenland (50°–30° W, 68°–78° N), atmospheric CO_2 and N_2O, and surface air temperature over Antarctica (68°–78° S). Inset, amplitude of N_2O changes versus the duration of corresponding stadials, from two ice-core records following ref. 15 (blue), and from four model simulations (orange).

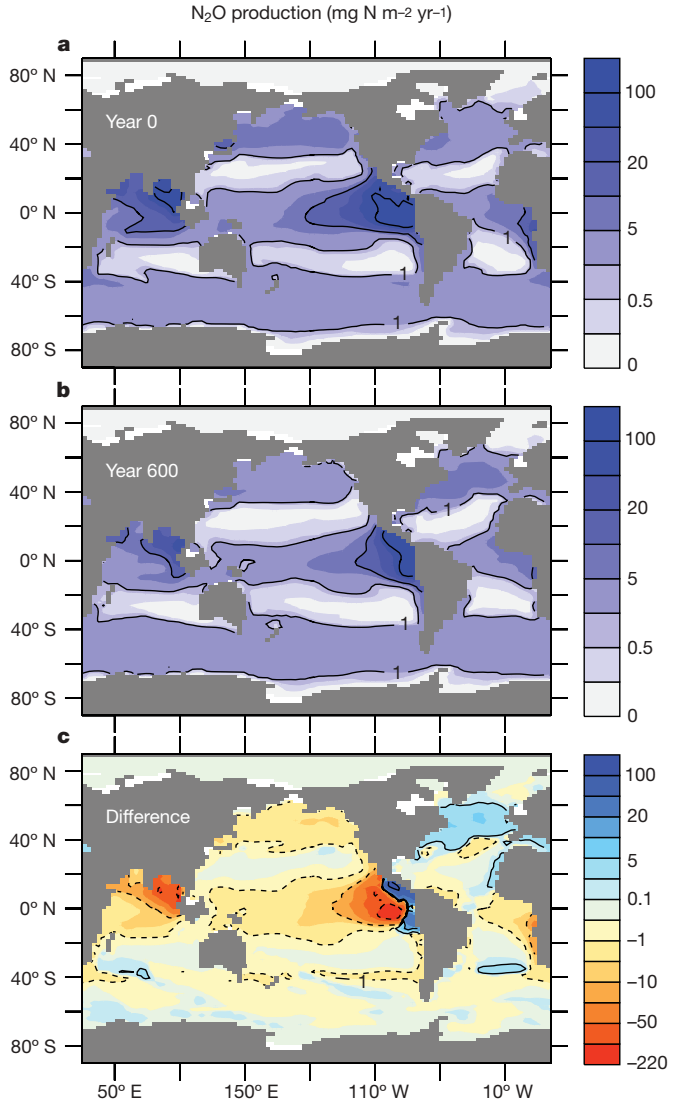

Figure 3 | Simulated ocean production of N_2O. **a**, During the interstadial at year 0; **b**, during the stadial at year 600; and **c**, the difference (year 600 minus year 0).

nonlinear dependence of N_2O production on oxygen concentrations, suggest that a zonally averaged model leads to a systematically biased underestimate. Sensitivity tests showed that the simulated amplitude is insensitive (<5%) to parameter uncertainties within their 1σ range of the empirical N_2O production equation[16], and that it is only moderately sensitive to the glacial ratio of marine to terrestrial N_2O production. Decreasing this ratio from 1/3 to 1/4 causes only a 15% reduction of the N_2O amplitude.

Methane variations on millennial timescales testify to changes in terrestrial systems during D-O events[17], which presumably also altered N_2O production rates to some degree. However, the history of N_2O changes recorded in ice cores is markedly different from that of methane[15], and the fact that our model can reproduce the correct amplitude of the glacial N_2O variations shows that changes in ocean sources could have dominated glacial variability of atmospheric N_2O on millennial timescales, obviating the need to invoke large changes in the terrestrial N_2O source[15,18].

The simulations also resolve a puzzling feature of the N_2O observations. Reference 15 notes that for long D-O oscillations, N_2O begins to increase before the rapid warming in Greenland, suggesting a lead and potentially a causal relationship for the AMOC resumptions. The simulations show a comparable lead, but our experimental set-up precludes N_2O effects on climate and hence N_2O variations cannot influence the model AMOC. Rather, the recovery of N_2O is related to the long-term adjustment of the upper-ocean nitrate and oxygen inventories after the AMOC collapse. After the initial decrease, upper-ocean nutrient levels and global productivity climb after year 600 (Supplementary Fig. 3), followed closely by N_2O production. Most of this increase occurs in the North Atlantic and Arctic oceans, as nutrient inventories in these basins slowly adjust to the altered circulation.

In contrast to N_2O, simulated CO_2 concentrations increase slowly by about 25 p.p.m.v., on a millennial timescale, after the AMOC shuts down (Fig. 1), and decrease again only after the AMOC has resumed, co-varying strongly with Antarctic temperature and ventilation in the Southern Ocean[19]. Despite an increase in terrestrial carbon on a millennial timescale, atmospheric CO_2 increases owing to a larger-amplitude decrease in the marine carbon inventory (Supplementary Fig. 1). This occurs despite a small increase in the solubility of CO_2 in the oceans[4,19], through a much larger reduction in the global efficiency of the oceanic biological pump, a mechanism which can be most clearly understood through the change in the ocean preformed nutrient inventory[20]. When surface waters in regions with high nutrient concentrations—principally the Southern Ocean—sink into the ocean interior, the capacity of those unutilized (preformed) nutrients to sequester carbon via the biological pump goes unrealized (Supplementary Fig. 2). In contrast, when nutrient-depleted waters from the subtropical Atlantic flow north to sink as NADW, they entrain relatively little preformed nutrients, thereby encouraging a higher efficiency of the biological pump[21]. A recently proposed theory quantitatively links changes in the atmospheric partial pressure of CO_2 (p_{CO_2}, in p.p.m.v.) to changes in the preformed fraction (P_{pref}/P_{tot}) of the global nutrient inventory[22]: $\Delta p_{CO_2} = 312 \times \Delta P_{pref}/P_{tot}$ (see Methods).

The quantity P_{pref}/P_{tot} is closely correlated with p_{CO_2} in our simulations (Fig. 1), increasing from 62% to more than 72% on a millennial timescale. The simple theory yields p_{CO_2} changes of ~30 p.p.m.v., somewhat overestimating the changes simulated by the complex model. The discrepancy arises mostly from simulated changes in land carbon, which decreases during the first 250 years, giving rise to the rapid initial increase in atmospheric CO_2 by 5 p.p.m.v., before reversing sign to gradually damp the long-term p_{CO_2} increase (Supplementary Fig. 1; see Supplementary Information for a discussion on uncertainties in land carbon simulations).

During the simulated shutdown of the AMOC, two factors conspire to cause the decreased efficiency of the biological pump, both of which relate to the volumetric contributions of water mass end-members to the ocean interior. First, diminished input of low-preformed-nutrient NADW to the deep ocean causes the ocean interior to gradually become more dominated by the high-preformed-nutrient waters of the Southern Ocean. Second, weakened Southern Ocean stratification, caused by reduced input of salt to the deep waters via NADW, allows more rapid production of waters with high preformed nutrients[19].

Modelled p_{CO_2} variations (Fig. 1) are ~25 p.p.m.v. for long D-O oscillations, consistent with ice-core data[23,24], and smaller for shorter oscillations, in agreement with previous results[19]. The simulation of small-amplitude p_{CO_2} changes during short D-O oscillations, which are likely to have been more influenced by terrestrial processes, cannot currently be evaluated because of the coarse time resolution of available p_{CO_2} data, but may be testable in the future as higher resolution data become available[23]. However, the simulated decrease of p_{CO_2} after the abrupt warming in Greenland is clearly faster than observed (Fig. 2; see also ref. 23). This discrepancy points to processes not captured by the model, such as the impact of wind-shift-induced precipitation changes on vegetation and land carbon storage[4] and/or ocean–sediment interactions, and indicates that more work needs to be done in order to fully reproduce the observed evolution of glacial CO_2 fluctuations on millennial timescales.

The simulations point to an important mechanistic contrast between the oceanic control on these two greenhouse gases (CO_2 and N_2O), explaining how contrasting atmospheric histories[15,23] can be generated through a unified oceanic process. The partial pressure of CO_2 gradually increases after the interstadial–stadial transition owing to release of carbon from the intermediate and deep ocean, related to changes in the global effectiveness of the biological pump[19]. The stadial decrease of N_2O, on the other hand, is much faster because it is controlled by adjustments of upper-ocean oxygen cycling. Our results emphasize the role of ocean circulation and biogeochemical cycling for atmospheric greenhouse-gas concentrations. Given model projections of slowing AMOC[25], and suggestions that the current ocean sink for carbon is already decreasing[26] and that the ocean source of N_2O might increase in the future[9], further progress in understanding ocean biogeochemical cycles will be required to refine the quantification of climate sensitivity to anthropogenic forcing.

METHODS SUMMARY

A two-dimensional (vertically averaged) energy-moisture-balance atmospheric model, including prescribed seasonally varying winds, provides a thermodynamically consistent solution for land–ocean surface conditions, without the computationally demanding requirements of a complex three-dimensional atmosphere. The model is well tested, and the ocean biogeochemical tracer distributions are in good agreement with observations when integrated under present-day conditions[9]. To improve comparison with the palaeorecord, we simulate aspects of the glacial climate by (1) prescribing land surface conditions in the presence of Northern Hemisphere (Laurentide and Fennoscandian) ice sheets[27] (that is, albedo, topography, no vegetation), and (2) increasing the outgoing long-wave radiation at the top of the atmosphere by 2.4 W m^{-2} (a simple approximation of reduced atmospheric greenhouse-gas concentrations). See Supplementary Information for details of the simulation of the glacial background climate.

Marine N_2O production was calculated from simulated oxygen concentrations and oxygen consumption rates using an empirical formula (equation (8) of ref. 16) that reflects both nitrification and denitrification pathways of N_2O production. N_2O production increases nonlinearly with decreasing oxygen concentrations, with most production in the oxygen-depleted regions of the thermocline in the eastern tropical Pacific and the northern Indian Ocean (Fig. 3). Terrestrial N_2O production and the stratospheric sink were assumed constant. See Supplementary Information for more details of the N_2O calculation.

The remineralized nutrient concentration is given by $P_{remi} = AOU \times R_{P:O}$, where AOU is the apparent oxygen utilization ($AOU = O_2^{sat} - O_2$), O_2 is the dissolved oxygen concentration in sea water, O_2^{sat} is the temperature dependent oxygen saturation concentration, and $R_{P:O}$ is a (constant) phosphorous to oxygen ratio. The efficiency of the biological pump can be expressed as the biologically sequestered fraction of the total nutrient inventory, $P_{remi}/P_{tot} = 1 - P_{pref}/P_{tot}$.

Received 29 April; accepted 30 September 2008.

1. Broecker, W. S., Peteet, D. R. & Rind, D. Does the ocean-atmosphere system have more than one stable model of operation? *Nature* **315,** 21–26 (1985).
2. Rahmstorf, S. Ocean circulation and climate during the past 120,000 years. *Nature* **419,** 207–214 (2002).
3. Stocker, T. F. Past and future reorganizations in the climate system. *Quat. Sci. Rev.* **19,** 301–319 (2000).
4. Menviel, L., Timmermann, A., Mouchet, A. & Timm, O. Meridional reorganizations of marine and terrestrial productivity during Heinrich events. *Paleoceanography* **23,** PA1203, doi:10.1029/2007PA001445 (2008).
5. Kohler, P., Joos, F., Gerber, S. & Knutti, R. Simulated changes in vegetation distribution, land carbon storage, and atmospheric CO_2 in response to a collapse of the North Atlantic thermohaline circulation. *Clim. Dyn.* **25,** 689–708 (2005).
6. Marchal, O., Stocker, T. F. & Joos, F. Impact of oceanic reorganizations on the ocean carbon cycle and atmospheric carbon dioxide content. *Paleoceanography* **13,** 225–244 (1998).
7. Scholze, M., Knorr, W. & Heimann, M. Modelling terrestrial vegetation dynamics and carbon cycling for an abrupt climatic change event. *Holocene* **13,** 327–333 (2003).
8. Goldstein, B., Joos, F. & Stocker, T. F. A modeling study of oceanic nitrous oxide during the Younger Dryas cold period. *Geophys. Res. Lett.* **30,** 1092, doi:10.1029/2002gl01418 (2003).
9. Schmittner, A., Oschlies, A., Matthews, H. D. & Galbraith, E. D. Future changes in climate, ocean circulation, ecosystems and biogeochemical cycling simulated for a business-as-usual CO_2 emission scenario until year 4000 AD. *Glob. Biogeochem. Cycles* **22,** GB1013, doi:10.1029/2007GB002953 (2008).
10. Meissner, K. J., Weaver, A. J., Matthews, H. D. & Cox, P. M. The role of land surface dynamics in glacial inception: a study with the UVic Earth System Model. *Clim. Dyn.* **21,** 515–537 (2003).
11. Schmittner, A., Saenko, O. A. & Weaver, A. J. Coupling of the hemispheres in observations and simulations of glacial climate change. *Quat. Sci. Rev.* **22,** 659–671 (2003).
12. Crowley, T. J. North Atlantic deep water cools the southern hemisphere. *Paleoceanography* **7,** 489–497 (1992).
13. Schmittner, A. Decline of the marine ecosystem caused by a reduction in the Atlantic overturning circulation. *Nature* **434,** 628–633 (2005).
14. Schmittner, A. *et al.* Large fluctuations of dissolved oxygen in the Indian and Pacific oceans during Dansgaard-Oeschger oscillations caused by variations of North Atlantic Deep Water subduction. *Paleoceanography* **22,** PA3207, doi:10.1029/2006PA001384 (2007).
15. Fluckiger, J. *et al.* N_2O and CH_4 variations during the last glacial epoch: Insight into global processes. *Glob. Biogeochem. Cycles* **18,** GB1020, doi:10.1029/2003GB002122 (2004).
16. Nevison, C., Butler, J. H. & Elkins, J. W. Global distribution of N_2O and the ΔN_2O-AOU yield in the subsurface ocean. *Glob. Biogeochem. Cycles* **17,** 1119 (2003).
17. Blunier, T. & Brook, E. J. Timing of millennial-scale climate change in Antarctica and Greenland during the last glacial period. *Science* **291,** 109–112 (2001).
18. Sowers, T., Alley, R. B. & Jubenville, J. Ice core records of atmospheric N_2O covering the last 106,000 years. *Science* **301,** 945–948 (2003).
19. Schmittner, A., Brook, E. J. & Ahn, J. in *Ocean Circulation: Mechanisms and Impacts — Past and Future Changes of Meridional Overturning* (eds Schmittner, A., Chiang, J. C. H. & Hemming, S. R.) 209–246 (Vol. 173, Geophysical Monograph Series, American Geophysical Union, 2007).
20. Sigman, D. M. & Haug, G. H. in *Treatise On Geochemistry* Vol. 6 (eds Holland, H. D. & Turekian, K. K.) 491–528 (Elsevier Science, 2003).
21. Toggweiler, J. R. *et al.* Representation of the carbon cycle in box models and GCMs — 2. Organic pump. *Glob. Biogeochem. Cycles* **17,** 1026, doi:10.1029/2001GB001401 (2003).
22. Ito, T. & Follows, M. J. Preformed phosphate, soft tissue pump and atmospheric CO_2. *J. Mar. Res.* **63,** 813–839 (2005).
23. Ahn, J. & Brook, E. J. Atmospheric CO_2 and climate on millennial time scales during the last glacial period. *Science* 322, 83–85 (2008).-.
24. Ahn, J. & Brook, E. J. Atmospheric CO_2 and climate from 65 to 30 ka BP. *Geophys. Res. Lett.* **34,** L10703, doi:10.1029/2007GL029551 (2007).
25. Schmittner, A., Latif, M. & Schneider, B. Model projections of the North Atlantic thermohaline circulation for the 21st century assessed by observations. *Geophys. Res. Lett.* **32,** L23710, doi:10.1029/2005GL024368 (2005).
26. Le Quere, C. *et al.* Saturation of the Southern Ocean CO_2 sink due to recent climate change. *Science* **316,** 1735–1738 (2007).
27. Peltier, W. R. Global glacial isostasy and the surface of the ice-age earth: The ICE-5G (VM2) model and GRACE. *Annu. Rev. Earth Planet. Sci.* **32,** 111–149 (2004).
28. Andersen, K. K. *et al.* High-resolution record of Northern Hemisphere climate extending into the last interglacial period. *Nature* **431,** 147–151 (2004).
29. EPICA. One-to-one coupling of glacial climate variability in Greenland and Antarctica. *Nature* **444,** 195–198 (2006).
30. Indermuhle, A. *et al.* Atmospheric CO_2 concentration from 60 to 20 kyr BP from the Taylor Dome ice core, Antarctica. *Geophys. Res. Lett.* **27,** 735–738 (2000).

Supplementary Information is linked to the online version of the paper at www.nature.com/nature.

Acknowledgements This study was funded by the NSF Marine Geology and Geophysics programme grant 0728315-OCE, and the NSF Paleoclimate programme grant 0602395-ATM. We thank J. Ahn, E. Brook, R. Toggweiler and V. Brovkin for discussions and comments on the manuscript.

Author Contributions A.S. designed the study and performed the numerical experiments. E.D.G. performed the comparison with the proxy record. A.S. and E.D.G. discussed the results and contributed equally to the analysis of the data and writing of the paper.

Author Information Reprints and permissions information is available at www.nature.com/reprints. Correspondence and requests for materials should be addressed to A.S. (aschmitt@coas.oregonstate.edu).